

# The Effect of Extrusion Processing Conditions on EVOH/Clay Nanocomposites at Low Organo-Clay Contents

N. Artzi, A. Tzur, M. Narkis

Department of Chemical Engineering, Technion – Israel Institute of Technology, Haifa 32000, Israel

A. Siegmann

Department of Materials Engineering, Technion – Israel Institute of Technology, Haifa 32000, Israel

Ethylene vinyl alcohol (EVOH) copolymer is studied as a host for low concentrations, up to 1 wt%, of organically treated clay. The clay develops a high interaction level with EVOH and thus high torque levels accompany the structuring process leading to the formation of nanocomposites. Extrusion residence time, successive extrusion passes, screw rotational speed, and processing temperature were all found to affect the morphology and the thermal and mechanical properties of the resulting composites. The extrusion compounded composites were subsequently injection molded. A subtle balance of processing parameters is required to achieve improved properties. Long extrusion residence times were found important for good clay dispersion in some cases, whereas in other cases an exfoliated structure was obtained already after the first extrusion pass. Two organically treated clay types processed at the same conditions were examined, and found to result in different morphology and mechanical behavior. Compression molding of extrusion compounded materials, under several extrusion conditions, was studied to illustrate the effect of shear level on the resulting morphology. The delamination level was higher after compression molding compared to that after injection molding. EVOH thermal properties and thermal stability of the related composites were also examined using differential scanning calorimetry and thermal gravimetric analysis. Higher extrusion processing temperature (220 compared to 200°C) was found to change the crystallization process of EVOH in the presence of clay, leading to significant decrease in  $T_m$  and  $T_c$  compared to that of the neat EVOH. POLYM. COMPOS., 26:343–351, 2005. © 2005 Society of Plastics Engineers

## INTRODUCTION

Polymer nanocomposites constitute a class of materials comprising a polymer matrix and an inorganic filler, which

has at least one dimension in the nanometer scale. Decreasing the particle size to the nano-size dimension influences the macroscopic properties and the common rule of mixtures is not obeyed. An extremely large amount of interfacial area is obtained and thus gains importance with respect to the bulk behavior [1].

Polymer/clay nanocomposites can be obtained by clay delamination and by polymer melt intercalation, where polymer chains diffuse into the space between the clay layers or galleries, followed by clay exfoliation. This approach can be realized by conventional polymer processing techniques, e.g., extrusion and injection molding, where polymer/clay hybrids are formed by breaking up clay particles and generating uniform dispersions. The amount of exfoliation appears to be strongly affected by the processing conditions. Generally, the level and mode of dispersion are governed by parameters such as matrix viscosity, level of shear field, and residence time in the process [2].

Polypropylene (PP)/clay composites are of commercial interest in the automotive industry. A few articles on PP/clay nanocomposites produced by melt mixing [3, 4] have been published. PP/clay composites showed significant enhancement in their mechanical properties by addition of just 4 wt% organo clay [3]. Another study showed a sharp increase of tensile strength from neat to 1 wt% clay, while further addition of clay improved only moderately the tensile strength [4]. The resulting properties of PP/clay nanocomposites were found to depend on processing conditions. Omachinski et al. [5] used a twin screw extruder for preparing PP/clay masterbatch that was then diluted with neat PP in a single screw extruder. Such composites showed better clay dispersion and mechanical properties than those prepared by direct compounding in a twin screw extruder [5]. In another study where PP/organoclay mixtures were compounded in a twin screw extruder, recompounding was found to ensure removal of visible tactoids from the extrudate [6].

Intercalation and/or delamination of organoclay when blended with ethylene vinyl alcohol copolymer (EVOH)

Correspondence to: M. Narkis; e-mail: narkis@tx.technion.ac.il

Contract grant sponsor: Israel Ministry of Science.

DOI 10.1002/pc.20096

Published online in Wiley InterScience (www.interscience.wiley.com).

© 2005 Society of Plastics Engineers

have been accomplished by melt mixing. The authors' previous studies [7–9] focused on compounding EVOH and clay in a Brabender plastograph mixing cell. The processing torque was found constant during the first 20 min of mixing followed by a gradual increase with mixing time, contrary to the neat EVOH, where a constant torque with mixing time was found. This was attributed to a fracturing process of the organoclay particles into smaller tactoids and delamination, leading to a dispersion of thin platelets in the nanometric scale within the EVOH matrix. Residence mixing time was found to strongly affect the structuring process of the composites, level of exfoliation, degree of EVOH crystallinity, and the resulting properties.

The present study addresses EVOH nanocomposites containing low clay concentrations by twin screw extrusion compounding and investigates their morphology (intercalation and/or exfoliation) and mechanical properties in relation to processing parameters such as processing temperature, residence time, and level of shear.

## EXPERIMENTAL

### Materials

The EVOH used is a commercial product (Kuraray, Japan) consisting of 32 mol% ethylene. Two types of organically treated clay were used: nanomer-I.30E, an onium ion surface modified montmorillonite mineral. The organically treated clay contains 70–75 wt% montmorillonite and 30–25 wt% octadecylamine. It is claimed to be designed for ease of dispersion in amine-cured epoxy resins to form nanocomposites. The second type was nanomer-I.35L, a surface modified montmorillonite mineral treated for EVOH resin. Both treated clays were obtained from Nanocor, IL.

### Preparation Methods

Prior to melt blending, the EVOH copolymer was milled into a powder. The polymer and clay powders were dried in a vacuum oven at 80°C and 60°C, for 15 hr each, respectively. The dried components were mixed at selected ratios, and processed in a counter rotating, intermeshing twin-screw extruder, Brabender TSC 42/6 (L/D = 6; D = 42 mm). The components were melt-mixed at two temperatures (200°C or 220°C in all zones), using two screw rotation speeds (20 and 40 rpm). Filaments of the various blends produced were ground and then injection molded using an Arburg 220/150 injection molding machine, equipped with an ASTM standard mold. The injection molding machine temperature was maintained at 200 or 220°C in all zones, and the mold at 40°C. Selected composites were compression molded after compounding (rather than injection molded) at the extrusion temperature (i.e., 200 or 220°C) for 15 min, under a pressure of 980 MPa, into 3-mm thick plaques.

### Characterization

**X-ray Diffractometer (XRD).** The layered structure of the clay was examined by a D/Max 2400, XRD, with a  $\text{CuK}\alpha$  radiation operated at 40 kV, 100 mA, and a scanning rate of 2°/min.

**Transmission Electron Microscope (TEM).** Philips CM120 TEM operated at 120 kV was used. The images were taken at a nominal underfocus of 4–7 nm, where any amplitude contrast is enhanced with phase contrast. Images were recorded digitally by a Gatan 791 MultiScan CCD camera using the Digital Micrograph 3.1 software package. The ultrathin sections were prepared at room temperature with a Reichert ULTRACUT E ultramicrotome, using a glass knife.

**Tensile Mechanical Properties.** Tensile properties of injection molded “dog bone” specimens were determined using an Instron 5568 universal testing machine, according to ASTM D 638-72. The initial gage length was 100 mm. The specimens were first extended at a low cross-head speed of 1 mm/min up to an extension of 0.5%, followed by a cross-head speed of 10 mm/min. An extensometer was used at the lower extension speed to accurately measure the strain. Five specimens were tested for each composite and the results averaged.

**Izod Impact.** Notched Izod impact resistance was determined using a Zwick 5102 pendulum impact tester, according to ASTM D 256-73. Impact test specimens were prepared using a 43-15-1 TMI notching cutter.

**Thermal Gravimetric Analysis (TGA).** TGA of the various EVOH/clay composites and the neat components was carried out using a TA 2050 TGA analyzer. Samples were heated under air atmosphere, at a heating rate of 20°C/min, monitoring their weight loss.

**Differential Scanning Calorimetry (DSC).** DSC was employed to characterize the thermal behavior of the composites. A Mettler DSC 30 system, under an inert nitrogen atmosphere, at a heating rate of 10°C/min was used. Samples were heated to a temperature above their melting, cooled at the same rate, and subsequently reheated. The melting behavior was determined from the second heating run.

## RESULTS AND DISCUSSION

### Twin Screw Extruder

EVOH/clay mixtures were processed by melt mixing in the counter rotating intermeshing Brabender twin screw extruder. The extrusion residence time was about 5 min and a constant torque with mixing time was monitored; how-

TABLE 1. Torque data in extrusion of EVOH/clay composites.

Composite	Torque (N*m)
200°C, 20 rpm	
Neat EVOH	45–50
EVOH+1% 1.35L, 1st pass	105–115
EVOH+1% 1.35L, 2nd pass	150–190
EVOH+1% 1.35L, 3rd pass	110–150
200°C, 40 rpm	
Neat EVOH	50
EVOH+0.5% 1.35L, 1st pass	90–110
EVOH+0.5% 1.35L, 2nd pass	110–130
EVOH+0.5% 1.35L, 3rd pass	130–150
EVOH+1% 1.35L, 1st pass	270
EVOH+1% 1.35L, 2nd pass	70
EVOH+1% 1.35L, 3rd pass	80
220°C, 40 rpm	
Neat EVOH	20
EVOH+1% 1.35L, 1st pass	23
EVOH+1% 1.35L, 2nd pass	23
EVOH+1% 1.35L, 3rd pass	30

ever, the torque levels were significantly higher compared with the neat EVOH in most experiments (Table 1).

A different behavior was observed by processing composites at 220°C, where a torque increase did not occur. According to the previous studies [7–9], the neat EVOH was found stable (constant torque) while processed at 230°C in a Brabender Plastograph cell for durations much longer than the extrusion average residence times and the torque was even increasing with mixing time when clay was added. In the present study, although the extrusion processing temperature is somewhat lower, i.e., 220°C, the high shear stresses developed in the extrusion process may lead to EVOH chain scission. The latter phenomenon seems to be triggered by the clay presence. In highly interacting systems containing a polar matrix, such as EVOH, the maximum clay content that can be incorporated is operationally limited. In the present study, the maximal permissible torque level enabled the use of up to 1 wt% clay. To explore the effect of residence time on the composites formed, the materials were reinserted into the extruder for three successive passes. Even after the first pass in the extruder, the torque was very high (Table 1), indicating that clay particles were fractured and exfoliated.

### XRD and TEM

X-ray and TEM are two complementary principal techniques for qualifying the degree of exfoliation or “dispersion” of the nanoparticles [10]. Therefore, X-ray results were supported by TEM, particularly the cases where no XRD characteristic basal reflection was obtained, which is indicative of exfoliated structure. Table 2 compares nanostructures of the composites prepared at different processing conditions, i.e., clay concentration, mixing temperature, screw rotational speed, and clay type, after each pass in the extruder and subsequent injection molding. XRD patterns of

TABLE 2. Structure of the EVOH/clay composites by XRD.

Composite	Extrusion conditions			
	Temperature (°C)	Speed (rpm)	Pass no.	Structure
EVOH+1% 1.35L	200	20	1st	Exfoliated
EVOH+1% 1.35L	200	20	2nd	Exfoliated
EVOH+1% 1.35L	200	20	3rd	Exfoliated
EVOH+0.5% 1.35L	200	40	1st	Exfoliated
EVOH+0.5% 1.35L	200	40	2nd	Exfoliated
EVOH+0.5% 1.35L	200	40	3rd	Exfoliated
EVOH+1% 1.35L	200	40	1st	Exfoliated
EVOH+1% 1.35L	200	40	2nd	Exfoliated
EVOH+1% 1.35L	200	40	3rd	Exfoliated
EVOH+1% 1.35L	220	40	1st	Intercalated
EVOH+1% 1.35L	220	40	2nd	Intercalated
EVOH+1% 1.35L	220	40	3rd	Intercalated
EVOH+1% 1.30E	200	40	1st	Intercalated
EVOH+1% 1.30E	200	40	2nd	Intercalated
EVOH+1% 1.30E	200	40	3rd	Intercalated

most of the composites containing 1.35L clay do not show a characteristic basal reflection, which is indicative of an exfoliated structure (which is verified by TEM). Exceptional are the composites prepared at 220°C (Fig. 1), where the characteristic reflections shown are indicative of an intercalated structure. Presumably the lower molecular weight of the EVOH leads to a lower melt viscosity and thus less stress transfer for platelets separation, in agreement with Fornes et al. [11]. Since individual platelets peel apart through a combination of shear stresses and diffusion of polymer chains into the clay galleries, reduction of stress transfer may lead to just intercalated structures. However, at the lower processing temperature, i.e., 200°C, where there is no indication of EVOH degradation, the combination of EVOH/clay high interaction and high levels of shear, may lead to individual platelets dispersion. The XRD pattern for the composite processed at 200°C and 20 rpm exhibited no clay reflections already after the first extrusion pass. The composite processed at 200°C and 40 rpm had an exfoliated structure (no characteristic basal reflection peak); however, the low reflection intensity after the first pass further decreases by the additional extrusion passes (Fig. 2). At 40 rpm the residence time is half of that at 20 rpm; hence, the longer residence times (second and third passes) result in higher delamination and platelets dispersion. A representative TEM micrograph is presented for EVOH containing 1 wt% clay processed at 200°C and 40 rpm, after first extrusion pass (Fig. 3). Individual platelets are embedded in the EVOH matrix and are marked with arrows. Figure 3a and b represents different regions from the sample. More regions were observed (not shown here), where the platelets were also completely dispersed, in agreement with the X-ray results showing no basal reflection.

To examine the effect of compression molding on the composite's structure, compounded pellets were compression molded into 3-mm thick plaques, at the extrusion temperature and under a pressure of 980 Mpa for 15 min. It

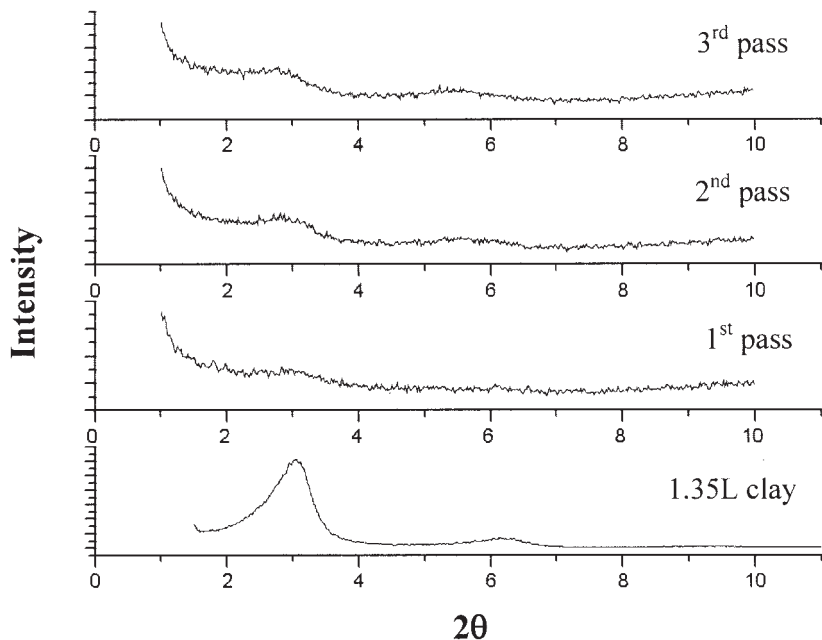


FIG. 1. XRD patterns of 99/1 EVOH/I.35L clay composite after first, second, and third extrusion passes at 220°C and 40 rpm, and injection molding at 220°C.

seems that the compression molding result was better in terms of clay dispersion relative to injection molding. Figure 4 depicts XRD patterns for EVOH containing 1 wt% 1.35L processed at 220°C and 40 rpm after the third extrusion pass, followed by either compression or injection molding. The neat 1.35L clay characteristic reflection is at 3° ( $d_{001} = 29 \text{ \AA}$ ). The corresponding reflection for the composite injection molded processed at 220°C is at 2.7° ( $d_{001} = 32 \text{ \AA}$ ). This reflection almost completely disappears when the composite is compression molded rather than injection molded, probably due to annealing effects. The effect of thermal treatment after extrusion was also studied

by Galgali et al. [12], who found that in extruded PP/clay nanocomposites the number of silicate layers in the tactoids decreased from six before annealing at 200°C to four after annealing.

When EVOH/I.30E clay was processed at 200°C and 40 rpm and then injection molded, only an intercalated structure was obtained (not shown here), in contrast to the exfoliated structure obtained for the 1.35L clay at the same conditions. The neat I.30E clay shows a characteristic reflection at  $2\theta = 3.6^\circ$  ( $d_{001} = 25 \text{ \AA}$ ). The incorporation of 1 wt% 1.30E clay into EVOH resulted in an intercalated structure with a gallery spacing of 32 Å ( $2\theta = 2.7^\circ$ ). The

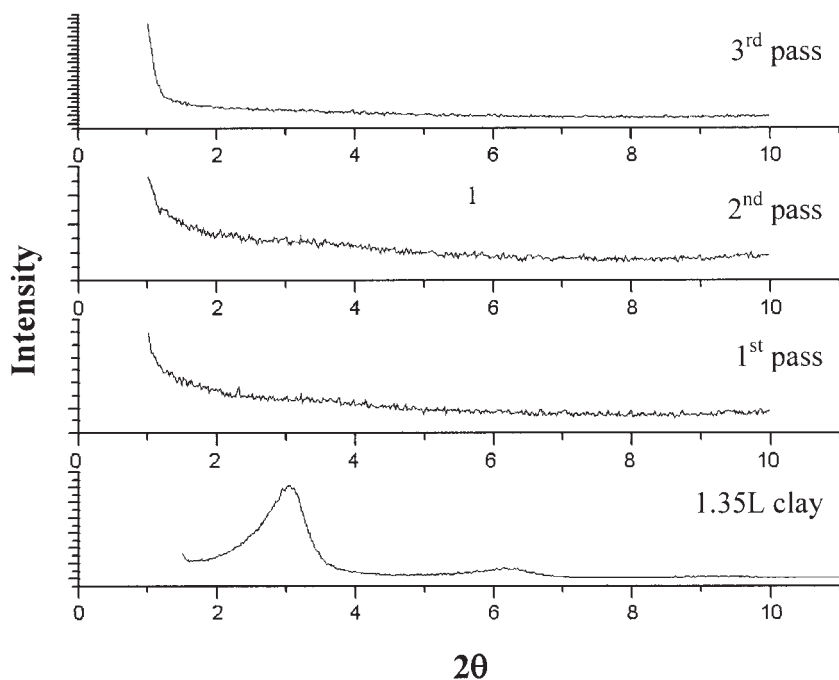


FIG. 2. XRD patterns of 99/1 EVOH/I.35L clay composite after first, second, and third extrusion passes at 200°C and 40 rpm, and injection molding at 200°C.



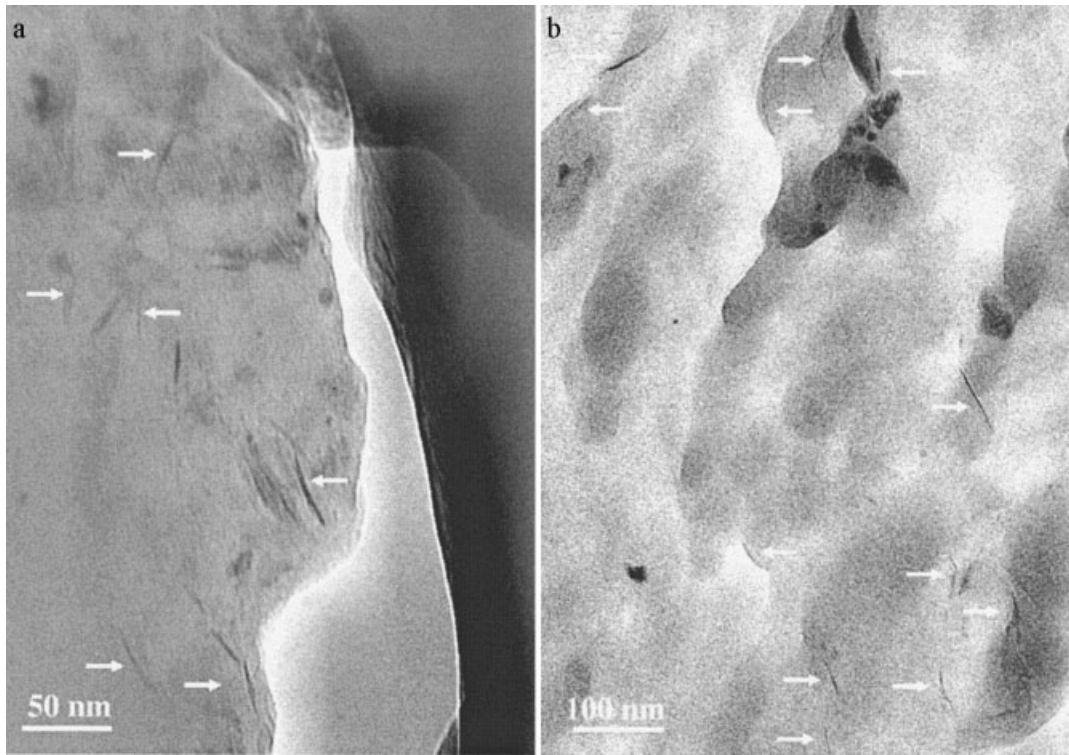


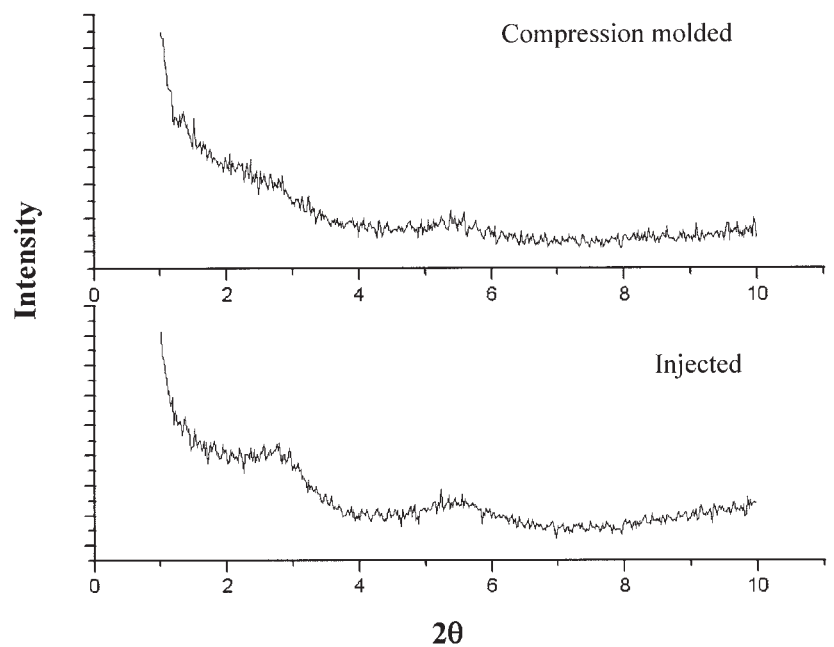
FIG. 3. TEM micrographs of 99/1 EVOH/clay composite after first extrusion pass at 200°C and 40 rpm, and injection molding at 200°C.

interaction level of the 1.30E clay with EVOH is lower than that of the 1.35L, in agreement with the authors' former study [8]. Less stress transfer and thus less platelets peeling is taking place in that case. However, by increasing the number of extrusion passes the delaminated fraction increases, as seen from the lower intensity and broadening of the clay characteristic reflection after the third extrusion pass.

#### Tensile Mechanical Properties

Typical stress-strain diagrams for EVOH and EVOH/clay composites processed at 200°C and 40 rpm are shown in Fig. 5 and their mechanical properties are summarized in Table 3. All composites exhibit a ductile fracture. For the composites processed at 200°C, regardless of clay type or content, the strength and modulus substantially increase

FIG. 4. XRD patterns of 99/1 EVOH/1.35L clay composite after third extrusion pass at 220°C and 40rpm, and injection molding or alternatively compression molding at 220°C.



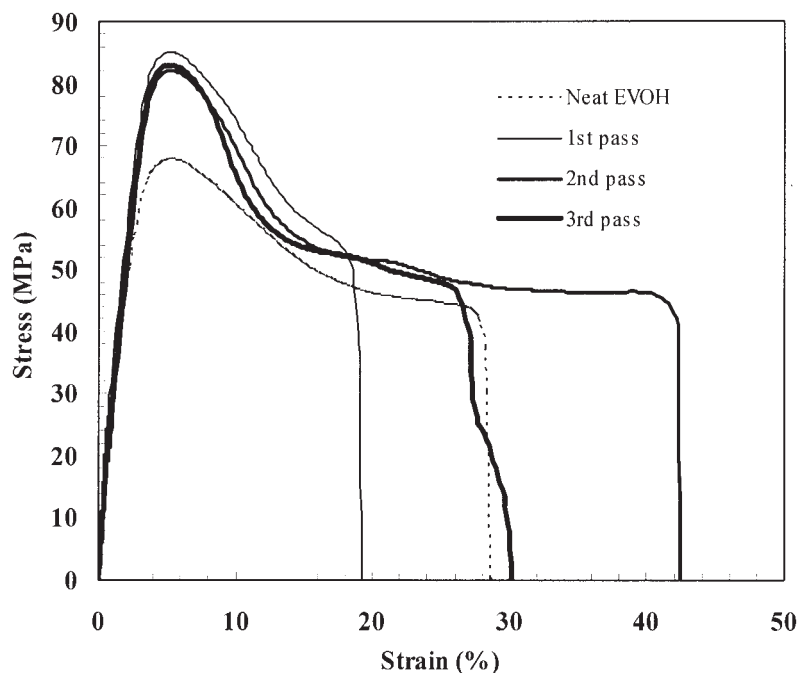


FIG. 5. Stress-strain curves of neat EVOH and 99.5/0.5 EVOH/1.35L clay composite after first, second, and third extrusion passes at 200°C and 40 rpm, and injection molding at 200°C.

relative to the neat EVOH, without impairing the Izod impact strength. The modulus and yield strength increase upon the addition of only 0.5 wt% 1.35L clay by 40 and 30%, respectively, under certain processing conditions (Table 3), which are significant increases for this low clay content. A literature article, for example, on PP/clay composites reports 10% modulus improvement by 1 wt% clay compared to the neat PP [4]. Additional extrusion passes slightly improve the EVOH composite strength when 1.30E clay is incorporated, in agreement with the increased delamination level according to the XRD results.

Upon processing at 220°C, the mechanical properties of the neat EVOH and the composites deteriorate except for the Izod impact strength, which remains practically constant. The EVOH modulus decreased by processing at 220°C compared to 200°C, probably owing to polymer thermo-mechanical degradation, in agreement with the low extrusion torque level developed by processing at 220°C. The EVOH degradation process is further enhanced in the presence of clay, leading to more reduction of modulus and strength. Elongation at break of the composite processed at 220°C is also low, presumably for the same reasons. In

TABLE 3. Selected mechanical properties of EVOH/clay nanocomposites.

EVOH/clay nanocomposites	Modulus (Mpa)	Yield strength (Mpa)	Elongation at yield (%)	Elongation at break (%)	Impact J/m
200°C, 40 rpm					
Neat EVOH	3490 ± 40	60 ± 10	4 ± 2	15 ± 2	61 ± 2
EVOH+0.5% 1.35L, 1st pass	4500 ± 200	83 ± 1	4.9 ± 0.2	18 ± 7	66 ± 3
EVOH+0.5% 1.35L, 2nd pass	4700 ± 300	83.7 ± 0.3	5.1 ± 0.1	18 ± 3	80 ± 10
EVOH+0.5% 1.35L, 3rd pass	4400 ± 300	83 ± 2	5.2 ± 0.2	22 ± 6	66 ± 4
EVOH+1% 1.35L, 1st pass	4100 ± 300	72 ± 1	5.20 ± 0.01	16 ± 2	61 ± 5
EVOH+1% 1.35L, 2nd pass	4200 ± 500	78 ± 1	5.40 ± 0.01	15 ± 4	62 ± 5
EVOH+1% 1.35L, 3rd pass	4020 ± 10	75 ± 1	5.40 ± 0.01	18 ± 4	70 ± 10
EVOH+1% 1.30E, 1st pass	4000 ± 200	75 ± 2	5.6 ± 0.2	70 ± 40	61 ± 8
EVOH+1% 1.30E, 2nd pass	4000 ± 300	78 ± 2	5.3 ± 0.2	12 ± 4	61 ± 5
EVOH+1% 1.30E, 3rd pass	4600 ± 100	82 ± 2	5.4 ± 0.1	20 ± 10	60 ± 10
200°C, 20 rpm					
Neat EVOH	3600 ± 300	66 ± 2	5.3 ± 0.1	40 ± 20	61 ± 2
EVOH+1% 1.35L, 1st pass	4500 ± 500	73 ± 1	5.1 ± 0.1	140 ± 30	77 ± 7
EVOH+1% 1.35L, 2nd pass	3900 ± 200	71 ± 2	5.5 ± 0.1	20 ± 2	67 ± 1
EVOH+1% 1.35L, 3rd pass	4100 ± 100	74 ± 1	5.5 ± 0.1	230 ± 60	65 ± 1
220°C, 40 rpm					
Neat EVOH	2120 ± 30	35 ± 1	4.7 ± 0.3	8 ± 2	32 ± 2
EVOH+1% 1.35L, 1st pass	1900 ± 100	35.5 ± 0.5	6.2 ± 0.2	8 ± 1	26 ± 2
EVOH+1% 1.35L, 2nd pass	1600 ± 100	34.5 ± 0.5	7.1 ± 0.2	8 ± 1	31 ± 3
EVOH+1% 1.35L, 3rd pass	1500 ± 100	34.5 ± 0.5	7.8 ± 0.2	9 ± 1	31 ± 2

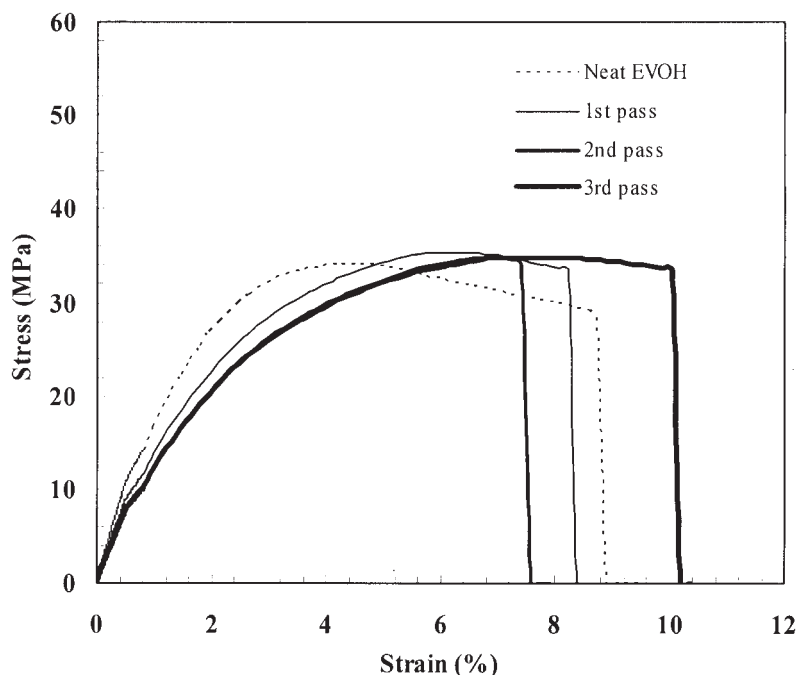


FIG. 6. Stress-strain curves of neat EVOH and 99/1 EVOH/I.35L clay composite after first, second, and third extrusion passes at 220°C and 40 rpm, and injection molding at 220°C.

addition, the presence of clay aggregates (evidenced by the XRD peak, Fig. 1) may also lead to reduction in elongation at break. Both EVOH and its composites processed at 220°C exhibit a relatively brittle fracture (Fig. 6) compared with the more ductile behavior of the composites processed at 200°C (Fig. 5). These results resemble the report of Fornes et al. [11], showing that composites based on nylon 6 of different molecular weights had different mechanical properties. The composite with low molecular weight, having an intercalated structure, has shown brittle fracture and lower modulus, elongation at break, and impact strength, compared to composites with medium and high molecular weights nylon 6, having an exfoliated structure, which have shown ductile fracture.

#### DSC

Recent studies [7–9] on EVOH nanocomposites have revealed that nano clays may hinder the crystallization process, owing to its high interaction level with EVOH, thus generating smaller EVOH crystals, having a lower melting temperature. However, in those studies 5–15 wt% clay loadings were used compared with 1 wt% clay or less in the present study. Literature articles report that the crystallization process of injection molded nylon 6 in the presence of 3–6 wt% clay yielded lower crystallinity levels and melting temperatures compared with the neat nylon 6 [13]. The presence of high concentrations of dispersed montmorillonite platelets hinders the formation of large crystalline domains due to the available limited space and in particular restrictions imposed on the movement of polymer chains by the high number of silicate platelets interacting with EVOH.

In the present study, where only 0.5–1 wt% clay is used,

no practical interruption to the EVOH crystallization process is seen, when the composites are processed at 200°C (Table 4). For the EVOH/I.35L clay, the crystallization temperature and melting temperature and enthalpy are essentially unaffected by the clay presence. However, when 1 wt% I.30E clay is used at 200°C and 40 rpm, the crystallization temperature is reduced by 6°C and the melting enthalpy by about 10 mJ/g (10% decrease), relative to the neat EVOH. Higher undercooling is required for crystallization resulting in lower degrees of crystallinity, whereas the melting temperature is similar to the neat EVOH. When the composites are extrusion processed at 220°C, the thermal properties change, even for the neat EVOH. Two crystallization temperatures, 123 and 161°C, and two melting temperatures, 162 and 181°C, appear for the EVOH extruded at 220°C. The higher  $T_c$  and  $T_m$  temperatures are similar to those of EVOH processed at 200°C (Table 4). When clay is incorporated, only the lower crystallization and melting temperatures at about 120 and 160°C, respectively, appear. The change of the neat EVOH thermal behavior in the presence of clay does not conform with the assumption that EVOH degrades at 220°C. Lower EVOH molecular weight should have imparted higher crystallization temperature. Therefore, the reduction in EVOH crystallization temperature should be a result of another mechanism interrupting the crystallization process. When EVOH is processed at high temperatures two competitive mechanisms may take place, namely thermal degradation and thus chain scission and grafting and oxidative cross-linking reactions [14].

The latter observed grafting and cross-linking could lead to the reduction of EVOH crystallization temperature. Hence, the main process of EVOH chain scission at 220°C is probably accompanied by low extent of grafting and

TABLE 4. Thermal properties for EVOH/clay nanocomposites.

EVOH/clay nanocomposites	T <sub>c</sub> (°C)	T <sub>m</sub> (°C)	ΔH <sub>m</sub> (mJ/g)
200°C, 20 rpm			
Neat EVOH	162	183	78
EVOH+1% 1.35L, 1st pass	164	183	84
EVOH+1% 1.35L, 2nd pass	165	182	82
EVOH+1% 1.35L, 3rd pass	157	182	78
200°C, 40 rpm			
Neat EVOH	163	182	82
EVOH+0.5% 1.35L, 1st pass	164	182	86
EVOH+0.5% 1.35L, 2nd pass	164	182	84
EVOH+0.5% 1.35L, 3rd pass	164	182	85
EVOH+1% 1.35L, 1st pass	164	182	85
EVOH+1% 1.35L, 2nd pass	164	182	84
EVOH+1% 1.35L, 3rd pass	163	182	85
EVOH+1% 1.30E, 1st pass	157	182	74
EVOH+1% 1.30E, 2nd pass	157	182	78
EVOH+1% 1.30E, 3rd pass	157	182	75
220°C, 40 rpm			
Neat EVOH	123, 161	162, 181	63, 10
EVOH+1% 1.35L, 1st pass	126	163	87
EVOH+1% 1.35L, 2nd pass	120	161	95
EVOH+1% 1.35L, 3rd pass	120	162	99

cross-linking. Another factor that could influence the crystallization process of EVOH is surface changes of the clay at the higher processing temperature (220 compared to 200°C). The possibility of degradation of the low molecular weight onium ions treating the clay was examined using TGA (not shown here). Heating the clay at 200 or 220°C for 30 min resulted in weight loss of only several percent, the same for both temperatures. Therefore, it is assumed that the main process altering the crystallization process of EVOH in the presence of clay at 220°C is the low extent of grafting and oxidative cross-linking reactions.

### TGA

Thermal stability of neat EVOH and EVOH/clay composites was examined by TGA under air atmosphere. Similar thermograms were obtained for neat EVOH and EVOH containing clay, both processed at 200°C. However, the thermograms of neat EVOH processed at 200 and 220°C, are significantly different (Fig. 7). The onset of weight loss temperature of EVOH processed at 200 and 220°C is 292 and 252°C, respectively. This result further supports the suggested EVOH molecular weight degradation when extrusion processed at 220°C. Another work on EVOH degradation under thermal oxidative conditions is reported by Lagaron and coworkers [15]. It was shown that EVOH weight loss is larger and also fastest at the first 2–3 min of heating for high conditioning temperature (215 compared to 200 and 190°C). The weight loss was accompanied by color formation. FTIR experiments suggested the formation of carbonyl groups, at the expense of OH groups, and some double bonds in the polymer chain.

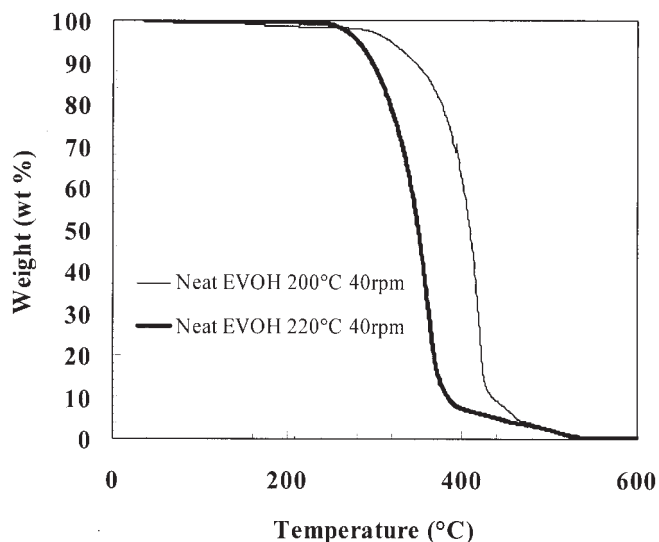


FIG. 7. TGA under air atmosphere of neat EVOH after extrusion and injection molding at 200 and 220°C.

### CONCLUSIONS

- 1) EVOH is a unique polymeric matrix for clay-nanocomposites owing to the strong EVOH/clay interactions developed.
- 2) Dynamic melt-mixing of EVOH/organoclay mixtures is accompanied by high torque levels owing to clay particle fracturing, intercalation, and delamination processes and the build-up of significant levels of polymer/clay interaction, thus requiring only very low clay contents for modification.
- 3) Mixed clay morphology of intercalation and delamination or complete exfoliation can be achieved, depending on blending conditions and clay type.
- 4) Processing conditions, temperature, and equipment, determine whether improved or deteriorated mechanical properties will result.
- 5) At low clay amounts, the interruption to EVOH crystallization is negligible in most of the processing conditions used, except for the composite processed at 220°C, where significantly lower  $T_m$  and  $T_c$  were obtained.

### ACKNOWLEDGMENT

N. Artzi acknowledges the generous Levi Eshkol scholarship from the Israel Ministry of Science.

### REFERENCES

1. E. van Zyl Werner, G. Monserrat, A.G.S. Bernard, J.K. Bart, Th.M. De Hosson Jeff, H. Verweij, *Macromol. Mater. Eng.*, **287**, 106 (2002).
2. J.W. Cho and D.R. Paul, *Polymer*, **42**, 1083 (2001).
3. P. Kodgire, R. Kalgaonkar, S. Hambir, N. Bulakh, and J.P. Jog, *J. Appl. Polym. Sci.*, **81**, 1786 (2001).



4. P. Svoboda, C. Zeng, H. Wang, L.J. Lee, and D.L. Tomasko, *J. Appl. Polym. Sci.*, **85**, 1562 (2002).
5. J. Omachinski, S. Qian, L. Tie, W.W. Timothy, and S.S. Walter, *60th ANTEC*, **1**, 214, 2002.
6. C. Ling, W. Shing-Chang, and P. Sreekumar, *J. Appl. Polym. Sci.*, **88**, 3298 (2003).
7. N. Artzi, Y. Nir, D. Wang, M. Narkis, and A. Siegmann, *Polym. Comp.*, **22**, 710 (2001).
8. N. Artzi, Y. Nir, M. Narkis, and A. Siegmann, *J. Polym. Sci., Part B: Polym. Phys.*, **40**, 1741 (2002).
9. N. Artzi, Y. Nir, M. Narkis, and A. Siegmann, *Polym. Comp.*, **24**, 627 (2003).
10. T.S. Ellis, *Polymer*, **44**, 6443 (2003).
11. T.D. Fornes, P.J. Yoon, H. Keskkula, and D.R. Paul, *Polymer*, **42**, 9929 (2001).
12. G. Galgali, C. Ramesh, and A. Lele, *Macromolecules*, **34**, 852 (2001).
13. T.D. Fornes and D.R. Paul, *Polymer*, **44**, 3945 (2003).
14. Y. Nir, "Structure and Properties Characterization of EVOH/Copolyamide 616.9 Blends," Ph.D. Thesis, Technion-IIT, Department of Chemical Engineering, Haifa, Israel (1996).
15. J.M. Lagaron, E. Giménez, and J.J. Saura, *Polym. Int.*, **50**, 635 (2001).